

First-principles investigation of exchange interactions in quasi-one-dimensional antiferromagnet CaV_2O_4

This content has been downloaded from IOPscience. Please scroll down to see the full text.

2015 J. Phys.: Condens. Matter 27 026001

(<http://iopscience.iop.org/0953-8984/27/2/026001>)

View [the table of contents for this issue](#), or go to the [journal homepage](#) for more

Download details:

This content was downloaded by: pchelkzl

IP Address: 195.19.154.70

This content was downloaded on 06/02/2015 at 08:54

Please note that [terms and conditions apply](#).

First-principles investigation of exchange interactions in quasi-one-dimensional antiferromagnet CaV_2O_4

Z V Pchelkina^{1,2} and I V Solovyev^{2,3}

¹ M N Miheev Institute of Metal Physics of Ural Branch of Russian Academy of Sciences, 620137, Ekaterinburg, Russia

² Theoretical Physics and Applied Mathematics Department, Institute of Physics and Technology, Ural Federal University, Ekaterinburg 620002, Russia

³ Computational Materials Science Unit, National Institute for Materials Science, 1-1 Namiki, Tsukuba, Ibaraki 305-0044, Japan

E-mail: pzv@ifmlrs.uran.ru

Received 23 October 2014

Accepted for publication 19 November 2014

Published 11 December 2014




CrossMark

Abstract

The effects of orbital degrees of freedom on the exchange interactions in a quasi-one-dimensional spin-1 antiferromagnet CaV_2O_4 are systematically studied. For this purpose a realistic low-energy electron model with the parameters derived from the first-principles calculations is constructed in the Wannier basis for the t_{2g} bands. The exchange interactions are calculated using both the theory of infinitesimal spin rotations near the mean-field ground state and the superexchange model, which provide a consistent description. The obtained behaviour of exchange interactions differs substantially from the previously proposed phenomenological picture based on magnetic measurements and structural considerations, namely: (i) despite the quasi-one-dimensional character of the crystal structure, consisting of the zigzag chains of the edge-sharing VO_6 octahedra, the electronic structure is essentially three-dimensional, that leads to finite interactions between the chains; (ii) the exchange interactions along the legs of the chains appear to dominate; and (iii) there is a substantial difference in exchange interactions in two crystallographically inequivalent chains. The combination of these three factors successfully reproduces the behaviour of experimental magnetic susceptibility.

Keywords: CaV_2O_4 , exchange interaction, low-dimensional magnetism, magnetic frustration, electronic structure, low-energy model

 Online supplementary data available from stacks.iop.org/JPCM/27/026001/mmedia

(Some figures may appear in colour only in the online journal)

1. Introduction

The CaV_2O_4 compound was studied both theoretically and experimentally owing to its low-dimensional magnetism and frustrated structure [1–3]. The high-temperature orthorhombic phase (the space group $Pnam$) undergoes a phase transition to the low-temperature monoclinic phase (the space group $P2_1/n11$) at $T_s \approx 141$ K. The main motif of both structures are the zigzag double chains of edge-sharing VO_6 octahedra (see figure 1). The distances between nearest and next-nearest

V neighbours are nearly equal, which, together with the antiferromagnetic (AFM) type of interactions, gives rise to geometrical frustrations. The electronic configuration of V^{3+} is $3d^2$, making CaV_2O_4 the appropriate compound for the investigation of $S = 1$ quasi-one-dimensional magnetism.

CaV_2O_4 has two crystallographically inequivalent types of vanadium atoms, V1 and V2, forming the zigzag chains. The vanadium atoms are displaced out of the center of the octahedra (see figure 1 of supplementary material (stacks.iop.org/JPCM/27/026001/mmedia)), yielding

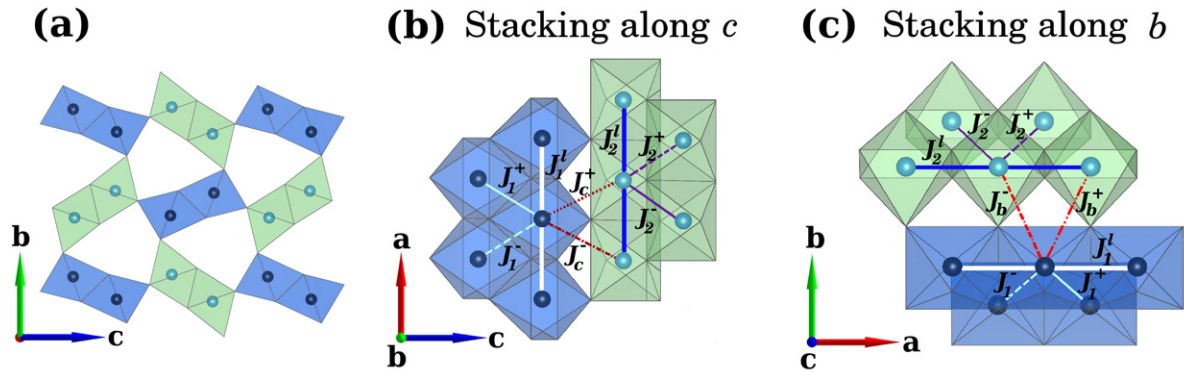


Figure 1. The crystal structure of the monoclinic phase of CaV_2O_4 in bc , ac and ba projections. Two nonequivalent V atoms are shown by dark blue (V1) and cyan (V2) spheres. The oxygen and calcium atoms are not shown for simplicity. The oxygen octahedra around V1 are coloured blue, while the octahedra around V2 are coloured light green. Each zigzag chain of vanadium atoms has two neighbouring chains of the other type, stacking along monoclinic directions c and b , as explained in panels (b) and (c), respectively. The definition of the main exchange interactions for each stacking is shown in (b) and (c). For visualization, the VESTA software [8] was used.

the existence of finite electric dipoles. However, both structures possess inversion symmetry, meaning that the dipoles are ordered antiferroelectrically. Each zigzag chain propagates along the a axis and has two neighbouring chains of the other type, which are stacked along the c and b axes (see figures 1(b) and (c), respectively). Each vanadium atom has six nearest vanadium neighbours forming six main exchange paths (the notations of corresponding interatomic distances are given in the brackets): J_1^l and J_2^l ($d_{1,2}^l$ and $d_{1,2}^l$)—along the ‘leg’ of the chain formed by V1 and V2, respectively; J_1^+ , J_1^- and J_2^+ , J_2^- (d_1^+ , d_1^- and d_2^+ , d_2^-)—along the zigzag in the positive and negative direction of a (denoted by ‘+’ and ‘-’, respectively); and two groups of interchain interactions along c and b : (J_c^+ , J_c^-) and (J_b^+ , J_b^-), respectively (see figure 1).

The magnetic structure of CaV_2O_4 has been studied already in the 1970s [4, 5] but it was impossible at that time to resolve the low-temperature monoclinic crystal structure and analyze correctly the experimental data. It is well known that below $T_N \approx 51\text{--}78\text{ K}$, the long-range antiferromagnetic order with the propagation vector $\mathbf{k} = (0, \frac{1}{2}, \frac{1}{2})$ sets in [2, 4–7]. The reduction of the ordered magnetic moment $1.0 \mu_B \leq m \leq 1.59 \mu_B$ (in comparison with $m = 2 \mu_B$ expected for $S = 1$) was detected in the ^{51}V nuclear magnetic resonance (NMR) measurements, muon-spin spectroscopy investigations, and powder diffraction [2, 4–7]. This reduction is typically attributed to low-dimensional and/or frustrated behaviour. The collinear spin orientation was found in the first neutron powder diffraction experiments at low temperatures [4, 5]. However, it was questioned in more recent NMR measurements [7] and the neutron diffraction experiments on high quality single crystals [3], which suggest some non-collinear spin arrangement.

Since the distances in the leg $d_{1,2}^l$ are nearly the same as in the zigzag $d_{1,2}^\pm$ (see figure 1) one could naively expect nearly equal exchange interactions $J_{1,2}^l \approx J_{1,2}^\pm$. However, the high-temperature dc susceptibility measurements on the CaV_2O_4 single crystals reveal that above T_s the system behaves like a $S = 1$ Heisenberg chain [3]. In order to explain this fact, it was typically assumed that (i) the zigzag chains, formed by V1 and V2, are nearly equivalent; and (ii) Three t_{2g} orbitals of

vanadium sites are oriented in such a way that their lobes are parallel to d^l , d^+ , and d^- , giving rise to the exchange paths J^l , J^+ , and J^- , respectively (J_{leg} , J_{zz}^l and J_{zz}^- in the notations of [3]).

In the orthorhombic phase, the lowest t_{2g} orbital was supposed to be occupied by one electron, while the second electron resides on a double degenerate level [3]. The direct overlap of the first orbitals leads to the strong AFM interaction along the leg (J^l), while the interactions in the zigzag are identical ($J^+ = J^-$) and should be considerably weaker than J^l . Hence, the system in the orthorhombic phase could be considered as a $S = 1$ Haldane chain. This scenario was supported by results of exact diagonalization calculations, supplemented with the fitting of the experimental high-temperature susceptibility data, which yield $J^l = -18.6\text{ meV}$ and $J^+ = J^- = -3\text{ meV}$ [3]. Nevertheless, in the same work [3], yet another scenario was proposed with $J^+ = J^- = -19.9\text{ meV}$ and $J^l = -0.8\text{ meV}$, which equally well fits the experimental data. In both cases, the fitting yields the Curie–Weiss temperature $\Theta = -418\text{ K}$ and the effective magnetic moment $\mu_{\text{exp}} = 2.77 \mu_B$ [3]. The negative value of Θ means that antiferromagnetic interactions in the system dominate.

Under the transition to the monoclinic phase, the additional distortions of the VO_6 octahedra completely lift the degeneracy of t_{2g} orbitals and make all exchange paths inequivalent. Moreover, the two t_{2g} orbitals are supposed to be occupied and the one orbital is empty, which should lead to the inequality $(J^l, J^+) \gg J^-$. Such a magnetic structure with the strong exchange couplings along the leg and every second interaction along the zigzag corresponds to a spin-1 ladder.

The above scenario was based solely on the qualitative structural consideration without taking into account the existence of the two nonequivalent types of vanadium atoms. Moreover, the assumed type of the orbital ordering was purely empirical and had no proper link to details of the crystal structure. In the present work we report theoretical investigation of the electronic structure, orbital ordering and exchange interactions in CaV_2O_4 . For this purpose

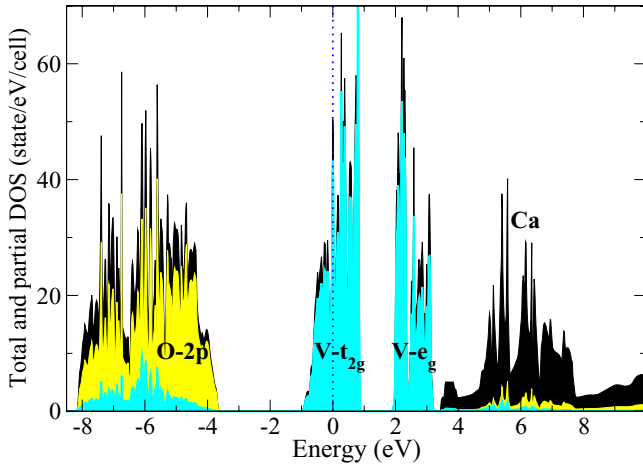


Figure 2. LDA total and partial densities of states for the monoclinic phase of CaV_2O_4 . Black, yellow, and cyan areas indicate, respectively, the total and partial O-2p and V-3d densities of states. The Fermi level (dotted line) is at zero energy.

we construct the realistic low-energy electron model and derive parameters of this model from the first-principles electronic structure calculations. Then we solve the model and obtain parameters of interatomic exchange interactions. The calculated values of exchange integrals are analyzed in the framework of the superexchange theory. The spin model with the calculated exchange parameters was solved by the quantum Monte-Carlo method in order to compare theoretical results with the experimental magnetic susceptibility.

2. Method

In order to analyze the electronic and magnetic properties of CaV_2O_4 , we employ the method of ‘realistic modeling’ (see [9] for a review). The same approach has been used in our previous theoretical study on the related compound NaV_2O_4 [10]. First, the band structure of CaV_2O_4 was calculated in the local density approximation (LDA). The total and partial densities of states (DOS) for the monoclinic phase are shown in figure 2. The bands located near the Fermi level have V- t_{2g} character. These bands are primarily responsible for the magnetic behaviour of CaV_2O_4 . Therefore, our next step is to concentrate on the behaviour of only these bands and to construct for them a realistic Hubbard-type model in the Wannier basis and derive all parameters of this model from the first-principles calculations. All the details of this procedure can be found in [9].

Most of the calculations reported in this work are performed for the experimental monoclinic $P2_1/n11$ structure (unless it is specified otherwise). We use the structure parameters from [11], but transform them to the conventional setting with the unique axis a and monoclinic angle β . The corresponding lattice parameters are $a = 2.99780 \text{ \AA}$, $b = 9.19524 \text{ \AA}$, $c = 10.68025 \text{ \AA}$, and $\beta = 90.767^\circ$. All atomic coordinates are summarized in the supplementary material (stacks.iop.org/JPCM/27/026001/mmedia).

To construct the model one needs to specify the three sets of parameters, namely, the crystal field (CF), transfer integrals,

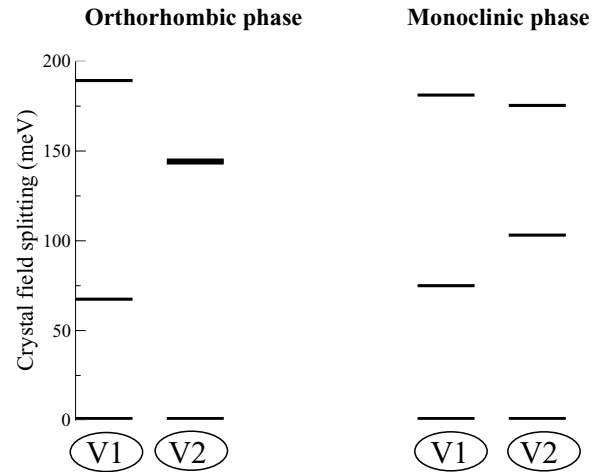


Figure 3. The crystal field splitting of the three t_{2g} states (in meV) for two types of V atoms in orthorhombic (left) and monoclinic (right) structures of CaV_2O_4 .

and screened Coulomb interactions. The CF splitting of the three t_{2g} levels for the orthorhombic and monoclinic structures is shown in figure 3. The relative position of atomic t_{2g} levels in the orthorhombic phase is (0, 67, 189) meV and (0, 143, 144) meV, while in the monoclinic phase it is (0, 75, 181) meV and (0, 103, 175) meV for V1 and V2, respectively. Thus, in the orthorhombic case two of the three levels of the V2 ion are almost degenerate while in the monoclinic phase this degeneracy is lifted by the additional distortion.

The arrangement of these three t_{2g} orbitals in the monoclinic phase of CaV_2O_4 corresponding to the aforementioned crystal field levels is illustrated in figure 4. In the following, for each vanadium site i (which can be either V1 or V2) we will denote the lowest, middle, and highest t_{2g} orbitals as ϕ_i^1 , ϕ_i^2 , and ϕ_i^3 , respectively.

The magnetic interactions are intimately connected with the spacial ordering of the t_{2g} orbitals [12]. Small structural distortions can lead to significant changes in the orbital ordering and magnetic properties of such compounds. In the monoclinic CaV_2O_4 , there are two d electrons occupying the lowest orbitals ϕ_i^1 and ϕ_i^2 . All VO_6 octahedra are compressed along the shortest V-O-V distance, which can be denoted as the local z axis and, for V1, almost coincides with the crystallographic c axis (see figure 1 in the supplementary material (stacks.iop.org/JPCM/27/026001/mmedia)). Then, the orbital of the xy symmetry should be the lowest in energy. Indeed all ϕ_i^1 orbitals have predominantly xy character in agreement with this simple structural consideration (see figure 4). The lobes of the ϕ_i^1 orbitals are pointed in the direction of neighbouring V ions, located along the leg of the zigzag chain. Hence, one could expect large transfer integrals in the legs of the zigzag chains.

The 3×3 matrices of the transfer integrals $t_{ij}^{mm'}$, calculated in the local CF representation are summarized in table 3 of the supplementary material (stacks.iop.org/JPCM/27/026001/mmedia). In these notations, i and j denote the vanadium sites, which can be of the type V1 or V2, while m runs over the CF orbitals ϕ_i^1 , ϕ_i^2 , and ϕ_i^3 . As expected, the largest transfer integrals operate between ϕ^1 orbitals in the

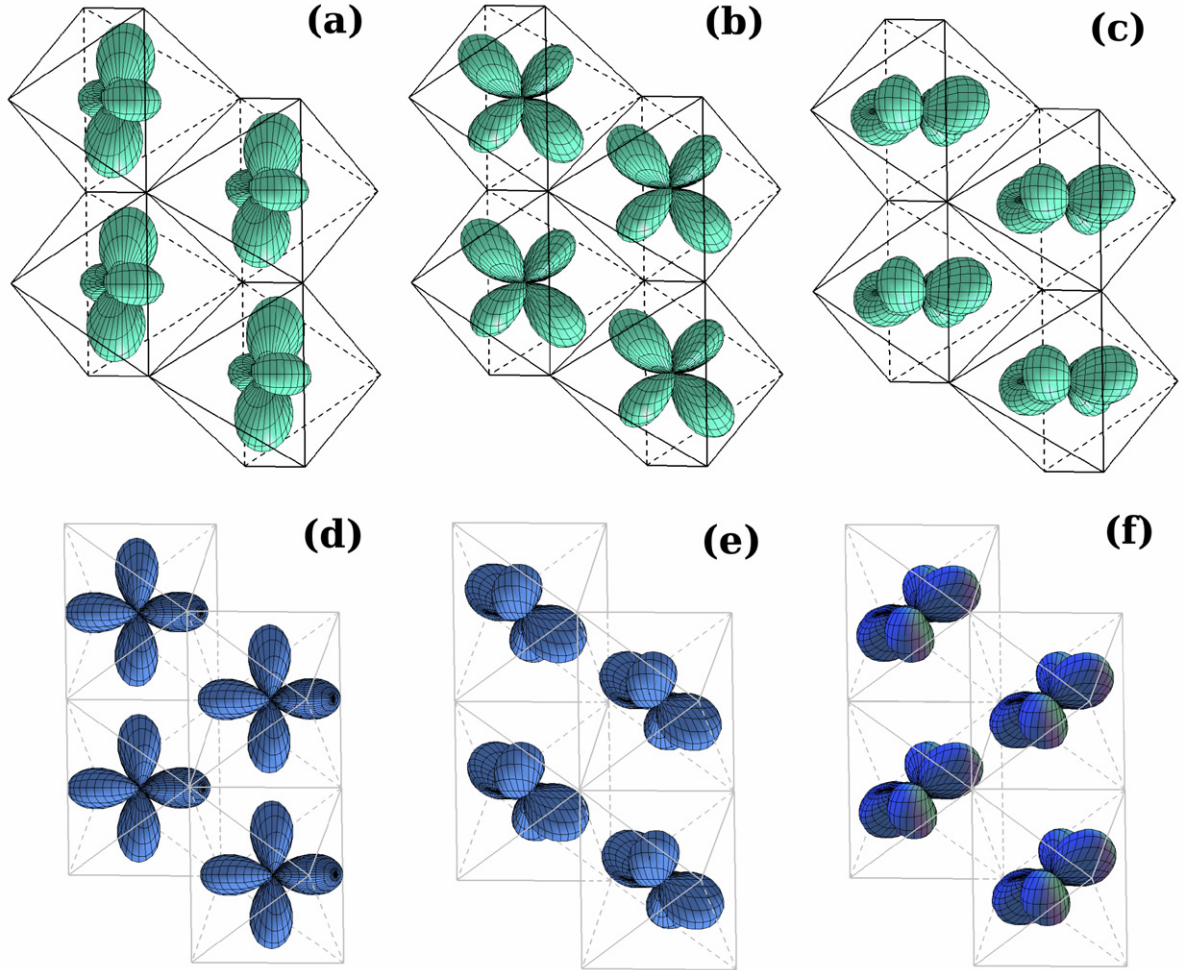


Figure 4. Three t_{2g} orbitals corresponding to the crystal field levels shown in figure 3 for the monoclinic phase of CaV_2O_4 . The orbitals (a)–(c) correspond to V1, while (d)–(f) correspond to V2. The orbitals are shown in order of increasing energies from left (the lowest in energy orbital) to right (the highest in energy orbital).

legs of the zigzag chains ($t_{ij}^{11} = -265$ and -233 meV for the chains formed by V1 and V2, respectively). The transfer integrals between the chains are weaker, but comparable with the intrachain ones. Thus, despite the quasi-one-dimensional character of the crystal structure, the transfer integrals in CaV_2O_4 are essentially three dimensional. The same trend has been found for related quasi-one-dimensional compound NaV_2O_4 [10].

In order to compute the screened Coulomb interactions in the t_{2g} band, we use the following procedure [9]. First, we apply the regular constraint LDA technique in order to consider the atomic screening of V-3d interactions by other electrons and take into account the effect of relaxation of the atomic V-3d orbitals. Then, the random-phase approximation (RPA) was employed in order to take into account the screening of V-3d electrons in the t_{2g} band by the same V-3d electrons, which participate in the formation of other bands due to the hybridization effects. The fitting of screened interactions in terms of two Kanamori parameters [13] results in the following values of the intraorbital Coulomb interaction $U = 3.42$ (3.46) eV and the intra-atomic exchange coupling $J_H = 0.63$ (0.64) eV for V1 (V2).

3. Results and discussion

3.1. Exchange interactions and magnetic ground state

First, we solve the obtained low-energy electron model in the mean-field Hartree–Fock approximation. For this purpose, we consider four collinear magnetic configurations, two of which, AFM2 and AFM3, were reported to be in moderate agreement with the single-crystal neutron diffraction data (see figures 5.29(a) and (b) in [3]). The unit cell was doubled along the a axis in order to arrange the V spin moments antiferromagnetically as was detected in the single-crystal neutron diffraction experiments [3, 11]. The sketch of the three considered AFM arrangements is shown in figure 5.

The parameters of interatomic magnetic interactions were calculated for different magnetic configurations by applying the perturbation theory expansion with respect to the infinitesimal spin rotations near the equilibrium state [9, 14]. This procedure corresponds to the *local* mapping of the total energy change associated with the small rotation of spins onto the Heisenberg model

$$H = - \sum_{i>j} J_{ij} \mathbf{e}_i \cdot \mathbf{e}_j, \quad (1)$$

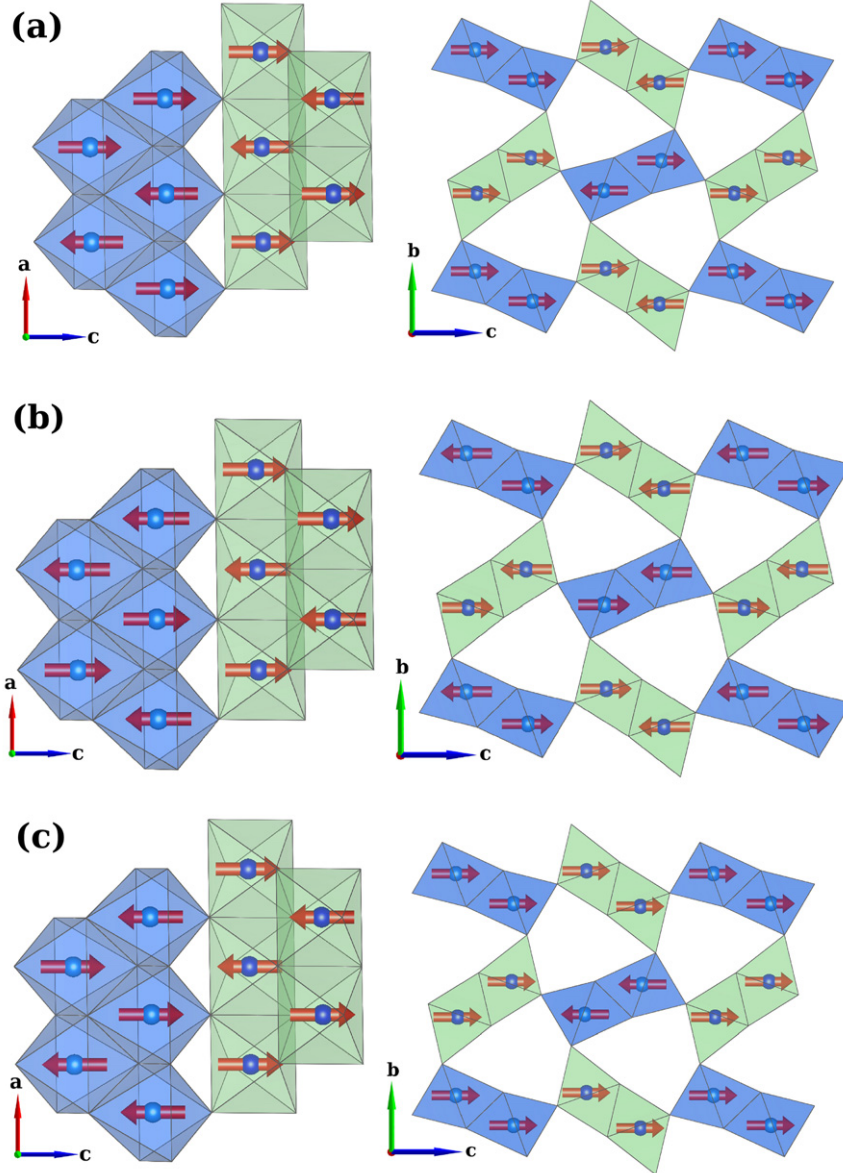


Figure 5. The sketch of different AFM configurations for the monoclinic phase of CaV_2O_4 in the cell, doubled along a axis: AFM1 (a), AFM2 (b) and AFM3 (c).

where \mathbf{e}_i is the direction of spin at the site i . The values of J_{ij} , obtained for the ferromagnetic (FM) and three AFM configurations, are summarized in table 4 of the supplementary material (stacks.iop.org/JPCM/27/026001/mmedia). The values obtained for the AFM3 configuration, which is found to be the magnetic ground state in the mean-field Hartree–Fock calculations without the spin–orbit coupling, are summarized in table 1. Since the degeneracy of t_{2g} orbitals is lifted by the lattice distortion, these exchange integrals only weakly depend on the type of the magnetic order in which they are calculated, which justifies the use of the spin-only model.

The leading antiferromagnetic exchange interactions $J_1^l = -19.9$ meV, $J_2^l = -13.9$ meV operate in the legs of the zigzag chains. They are about 7 times larger than other interactions in the system. The parameters of the antiferromagnetic interactions in the zigzag-rung are $J_1^+ = -1.3$ meV, $J_1^- = -0.4$ meV and $J_2^+ = -1.6$ meV,

$J_2^- = -1.6$ meV for V1 and V2, respectively. Such behaviour corresponds to the limit $J^l \gg J^\pm$, which is consistent with the analysis of experimental magnetic susceptibility data [3]. Nevertheless, the interactions J_1^l and J_2^l in two different types of chains differ substantially from each other.

The interactions between different types of the zigzag chains along c direction are ferromagnetic: $J_c^+ = 1.1$ meV and $J_c^- = 2.9$ meV. Similar interactions along b are found to alternate: $J_b^+ = -1.3$ meV is antiferromagnetic, while $J_b^- = 1.5$ meV is ferromagnetic. Such interactions should stabilize the AFM3 phase. These results are totally consistent with direct Hartree–Fock calculations, where the AFM3 state was found to have the lowest energy.

In order to get some insight into the microscopic origin of the exchange interactions, one can estimate the parameters in the superexchange approximation, starting from the atomic limit and considering virtual hoppings to the neighbouring sites

Table 1. Comparison of exchange integrals obtained in the Hartree–Fock calculation for the AFM3 state, $J(\text{HF})$, with results of the superexchange theory, $J(\text{SE})$, and available experimental estimates of J 's from the inelastic neutron scattering, $J(\text{INS})$, [11] and the magnetic susceptibility data, $J(\text{SC})$, [2, 3]. Two sets of exchange interactions reported in [3] correspond to two possible solutions, which cannot be distinguished by the fitting of the magnetic susceptibility. All values are in meV.

	$J(\text{HF})$	$J(\text{SE})$	$J(\text{INS})$ [11]	$J(\text{SC})$ [2]	$J(\text{SC})$ [3]
J_1^l	-19.9	-19.7	-30.0	0	-0.8/-18.6
J_2^l	-13.9	-12.6	-30.0	0	-0.8/-18.6
J_1^+	-1.3	-1.4	-11.0	-19.8	-19.9/-3.0
J_1^-	-0.4	-1.4	-7.9	-19.8	-19.9/-3.0
J_2^+	-1.6	-1.7	7.8	-19.8	-19.9/-3.0
J_2^-	-1.6	-4.9	5.7	-19.8	-19.9/-3.0
J_c^+	1.1	0.2	-2.0	$J_\perp \geq 0.8$	
J_c^-	2.9	4.2	-2.0		
J_b^+	-1.3	0.3	-1.5		
J_b^-	1.5	2.3	-1.5		

in the first order of $1/U$ [12, 15]. Then, J_{ij} can be calculated as the energy difference between FM ($\uparrow\uparrow$) and AFM ($\uparrow\downarrow$) configurations of spins in the bond ij : $J_{ij} = (E_{ij}^{\uparrow\downarrow} - E_{ij}^{\uparrow\uparrow})/2S^2$, where $S = 1$. Since $O-2p$ and $V-t_{2g}$ bands are separated by the large energy gap (see figure 2), we consider only the interactions caused by the effective transfer integrals $t_{ij}^{mm'}$ and neglect the direct contribution of the oxygen states. In the case of CaV_2O_4 , there are two electrons residing on six spin-orbitals of t_{2g} symmetry. Therefore, in the atomic limit, two majority-spin orbitals ϕ^1 and ϕ^2 are occupied and all other orbitals (such as majority-spin ϕ^3 and all minority-spin orbitals) are empty. Then, taking into account that the hoppings are allowed only between orbitals with the same spin, we will have:

$$E_{ij}^{\uparrow\uparrow} = -\frac{t_{ij}^{13}t_{ji}^{31} + t_{ij}^{23}t_{ji}^{32}}{U - 3J_H} + (i \leftrightarrow j) \quad (2)$$

and

$$E_{ij}^{\uparrow\downarrow} = -\frac{t_{ij}^{11}t_{ji}^{11} + t_{ij}^{22}t_{ji}^{22}}{U} - \frac{t_{ij}^{12}t_{ji}^{21} + t_{ij}^{21}t_{ji}^{12} + t_{ij}^{13}t_{ji}^{31} + t_{ij}^{23}t_{ji}^{32}}{U - 2J_H} + (i \leftrightarrow j). \quad (3)$$

The exchange integrals, calculated using the values of transfer integrals from table 3 of the supplementary material (stacks.iop.org/JPCM/27/026001/mmedia) (note that $t_{ij}^{mm'} = t_{ji}^{m'm}$) and the parameters of on-site Coulomb (U) and exchange (J_H) interactions, are summarized in table 1. For example, for the leg of the V1 chain one obtains: $E^{\uparrow\uparrow} = -3.34$ meV and $E^{\uparrow\downarrow} = -42.75$ meV. Therefore, $J_1^l(\text{SE})$ in the superexchange approximation can be estimated as $J_1^l(\text{SE}) = -19.7$ meV, which is in excellent agreement with $J_1^l = -19.9$ meV, obtained using the theory of infinitesimal spin rotations. For the V2 chain one obtains: $E^{\uparrow\uparrow} = -12.65$ meV and $E^{\uparrow\downarrow} = -37.89$ meV, which yield $J_2^l(\text{SE}) = -12.6$ meV, being in good agreement with $J_2^l = -13.9$ meV, derived from the theory of infinitesimal spin rotations. Hence, the difference between leading exchange integrals for two nonequivalent types of vanadium atoms reflects the behaviour of transfer integrals. The analysis for other bonds ij can be performed in a similar way (see table 1 of the main text and table 3 of the supplementary material (stacks.iop.org/JPCM/27/026001/mmedia)). In general, we obtain a good agreement between results of the superexchange theory and those of the infinitesimal spin rotations.

The experimental estimations of the exchange interactions in CaV_2O_4 have been performed in two ways. On the one hand, the high temperature susceptibility data have been fitted using the $S = 1$ chain model with the nearest-neighbour and next-nearest-neighbour interactions. In notations of our paper, they corresponds to J^\pm and J^l , respectively. The solution of this model using the exact diagonalization method leads to the $J^\pm(\text{SC}) = -19.82$ meV and $J^l(\text{SC}) = 0$ [2], which corresponds to the linear $S = 1$ Haldane chains. The coupling between these chains was estimated to be $J_\perp/J^\pm \gtrsim 0.04$, which corresponds to $|J_\perp(\text{SC})| \gtrsim 0.8$ meV. Shortly after, similar fitting revealed two possible solutions with $J^\pm(\text{SC}) = -19.85$ meV, $J^l(\text{SC}) = -0.75$ meV and $J^\pm(\text{SC}) = -3.02$ meV, $J^l(\text{SC}) = -18.60$ meV [3]. In fact, these two solutions are magnetically equivalent: in the first case $J^\pm(\text{SC})$ prevails and the single spin-1 chain is realized, while in the second case $J^l(\text{SC})$ is dominant, which corresponds to the formation of two independent spin-1 chains. This illustrates the fact that the fitting of the magnetic susceptibility data for materials with competing magnetic interactions is not unique: different sets of parameters can lead to similar behaviour of the susceptibility. The inelastic neutron scattering measurements of the magnetic excitation spectrum might settle this issue.

The comprehensive analysis of the complex spin wave spectrum, obtained by the inelastic neutron scattering (INS) technique [11] for the low-temperature monoclinic phase of CaV_2O_4 has enabled us to determine ten exchange parameters as well as the values of single-ion anisotropy for nonequivalent V ions. The best fit to experimental INS data was obtained for the following set of exchange interactions: $J_1^l(\text{INS}) = J_2^l(\text{INS}) = -30$ meV, $J_1^+(\text{INS}) = -11$ meV, $J_1^-(\text{INS}) = -7.9$ meV, $J_2^+(\text{INS}) = 7.8$ meV, $J_2^-(\text{INS}) = 5.7$ meV [11]. The full set of parameters is listed in table 1, in comparison with results of the present work and the magnetic susceptibility data. The inelastic neutron scattering data reveal that the leading exchange interaction is along the leg of the zigzag chains, which partly resolves the controversy with the fitting of magnetic susceptibility data. However, the value of the leg coupling $J^l(\text{INS}) = -30$ meV, obtained in the neutron scattering [11], is about 40% larger than the one derived from the fitting of the susceptibility data $J^l(\text{SC}) = -18.6$ meV [3].

Moreover, the exchange interactions in zigzag rungs are rather strong, $|J_{1,2}^{\pm}(\text{INS})| \approx 5.7\text{--}11$ meV, in comparison with the values $|J^{\pm}(\text{SC})| = 3$ meV, derived from the susceptibility fitting. Thus, it is clear that there is some controversy in the analysis of exchange interactions obtained from the magnetic susceptibility and inelastic neutron scattering measurements.

To summarize this section, our theoretical value of the exchange integral $J_1^l = -19.9$ meV (for the V1 chain) is in excellent agreement with the value obtained by the fitting of susceptibility data [2, 11]. Although calculated exchange parameters $|J_{1,2}^{\pm}| \approx 0.4 \div 1.6$ meV are somewhat smaller than those estimated from the susceptibility fitting $|J^{\pm}(\text{SC})| = 3.02$ meV, the general tendency $|J_{1,2}^l| \gg |J_{1,2}^{\pm}|$ is maintained. The exchange interaction between different zigzag chains $|J_{b,c}^{\pm}| \approx 1.05 \div 2.9$ meV are consistent with the estimation based on the susceptibility fitting $J_{\perp} \approx 1$ meV [11]. Nevertheless, our theoretical calculations reveal a strong difference in exchange interactions in the legs of two crystallographically inequivalent chains: $J_1^l = -19.9$ meV and $J_2^l = -13.9$ meV. It is worth mentioning that the experimental and theoretical exchange interactions seem to provide evidence against the ladder model ($J^l, J^+ \gg J^-$) for the monoclinic phase of CaV_2O_4 .

3.2. Susceptibility

In order to compare the obtained values of the exchange interactions with the experimental data, we first solve the next-nearest-neighbour spin-1 chain Heisenberg model separately for V1 and V2 using the exact diagonalization (ED) method implemented in the ALPS simulation package [16]. In these calculations, for the nearest-neighbour interactions in the chain i , we use the averaged value of J_i^+ and J_i^- ; and for the next-nearest-neighbour interactions, we use J_i^l . By doing so, we actually simulate the behaviour of the orthorhombic phase, which is realized above 141 K and for which $J_i^+ = J_i^-$. The $L = 12$ spins along the chain were taken into account. The results are summarized in figure 6. From figure 6(a) one can see that the behaviour of the single V1 chain with the leading exchange $J_1^l = -19.9$ meV agrees with experimental data very well. This finding is consistent with the results of [3]. Since the $J_2^l = -13.9$ meV is substantially smaller than J_1^l , the susceptibility for the V2 chain is overestimated. By considering these two noninteracting with each other zigzag chains, the total susceptibility should be obtained by averaging the data for the individual chains. Because of the V2 contribution, the obtained susceptibility deviates considerably from the experimental one (see figure 6(b)), indicating that probably the model of two noninteracting alternating chains is not appropriate for CaV_2O_4 .

Then, we try to take into account the interactions between different chains and solve a more complex model using the quantum Monte-Carlo method implemented in the ALPS simulation package [16, 17]. Because of the complexity of the problem (the existence of two inequivalent chains and different types of interactions between the chains) we have to rely on additional simplifications. First, we neglect the contributions of small and alternating (FM and AFM)

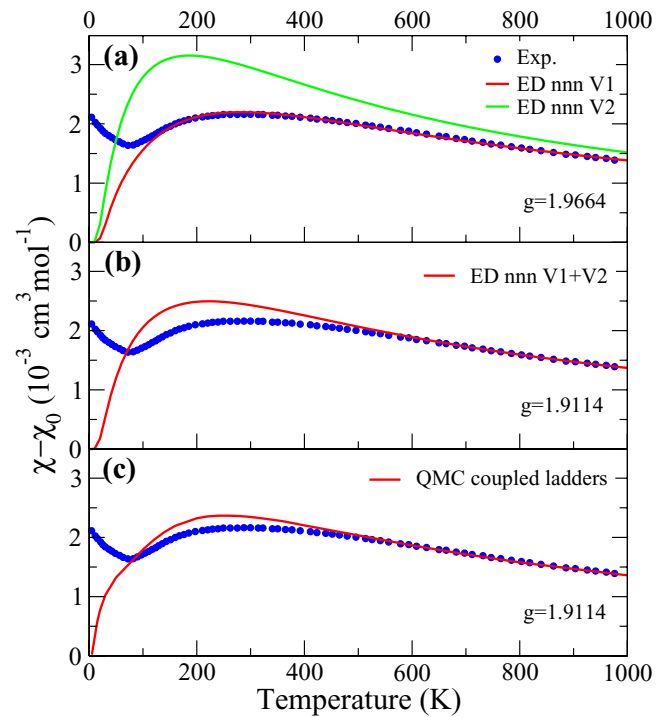


Figure 6. The comparison of experimental static magnetic susceptibility $\chi - \chi_0$ (where $\chi_0 = 0.48 \times 10^{-3} \text{ cm}^3 \text{ mol}^{-1}$ is the temperature-independent contribution) from [3, 11] (shown by blue dots) with the solution of the Heisenberg model using calculated values of exchange interactions. Panel (a): results for two separate noninteracting chains of V1 and V2 (red and green curves, correspondingly). Panel (b): the averaged susceptibility, obtained using the data for noninteracting chains (red curve). Panel (c): results for the coupled ladders model (red curve).

interactions J_b^{\pm} . As a result, the problem is reduced to the analysis of a two-dimensional model. Then, we consider the ladders, consisting of two different interactions, J_1^l and J_2^l , in two legs of this ladder, and take into account the strongest interchain interaction $J_c^- = 2.9$ meV as the rung of the ladder. Finally, we consider the interaction between these ladders. For this purpose we use the average value of four parameters: J_1^+ , J_1^- , J_2^+ , and J_2^- . The results of these simulations are shown in figure 6(c). The considered two-dimensional model substantially improves the agreement with the experimental data and reproduces the wide peak of susceptibility at around 250 K. The values of the g -factor (1.996 and 1.911), obtained from the fitting of calculated susceptibility to the experimental data are within the typical data range $1.92 \leq g \leq 2.00$ used for the vanadium compounds and the value 1.958 obtained from the Curie–Weiss fitting of the experimental susceptibility in [3].

4. Conclusions

The electronic structure, orbital configuration and magnetic interactions of quasi-one-dimensional antiferromagnet CaV_2O_4 was studied. For this purpose, the realistic Hubbard-type model for t_{2g} bands has been constructed with all the parameters derived from the first-principles calculations in the Wannier basis. The crystal field splitting and orbital ordering

are found to be different for two types of crystallographically inequivalent vanadium atoms. This affects the behaviour of interatomic exchange interactions, which is found to be different, in several respects, from the phenomenological picture, based on the analysis of the crystal structure of CaV_2O_4 and the fitting of the experimental magnetic susceptibility data. In particular, we have found that the exchange interactions in two crystallographically inequivalent zigzag chains behave rather differently. Furthermore, there is a substantial interaction between the zigzag chains, which is comparable with intrachain interactions. This analysis allowed us to resolve several controversial issues regarding the leading exchange interactions in CaV_2O_4 and the relative roles played by the intrachain and interchain interactions. Moreover, we argue that the interaction between the zigzag chains is an important ingredient of the realistic spin model, which should be taken into account, for instance, in the analysis of magnetic susceptibility data.

Acknowledgments

The authors thank Professor D C Johnston, B Lake and O Pieper for providing the comprehensive information on crystal and magnetic structure of CaV_2O_4 . This work was supported by the project 14-12-00306 of the Russian Science Foundation. Some of the calculations were performed on the ‘Uran’ cluster of the IMM UB RAS.

References

- [1] Kikuchi H, Chiba M and Kubo T 2001 *Can. J. Phys.* **79** 1551
- [2] Niazi A *et al* 2009 *Phys. Rev. B* **79** 104432
- [3] Pieper O *et al* 2009 *Phys. Rev. B* **79** 180409
- [4] Bertaut E F, van Nhung N and Hebd C R 1967 *Seances Acad. Sci. B* **264** 1416
- [5] Hastings J M, Corliss L M, Kunnmann W and La Placa S 1967 *J. Phys. Chem. Solids* **28** 1089
- [6] Sugiyama J, Ikedo Y, Goko T, Ansaldo E J, Brewer J H, Russo P L, Chow K H and Sakurai H 2008 *Phys. Rev. B* **78** 224406
- [7] Zong X, Suh B J, Niazi A, Yan J Q, Schlager D L, Lograsso T A and Johnston D C 2008 *Phys. Rev. B* **77** 014412
- [8] Momma K and Izumi F 2011 *J. Appl. Crystallogr.* **44** 1272
- [9] Solovyev I V 2008 *J. Phys.: Condens. Matter.* **20** 293201
- [10] Pchelkina Z V, Solovyev I V and Arita R 2012 *Phys. Rev. B* **86** 104409
- [11] Pieper O 2010 *PhD Thesis* Der Technischen Universitt Berlin
- [12] Kugel K I and Khomskii D I 1982 *Sov. Phys.—Usp.* **25** 231
- [13] Kanamori J 1963 *Prog. Theor. Phys.* **30** 275
- [14] Liechtenstein A I, Katsnelson M I, Antropov V P and Gubanov V A 1987 *J. Magn. Magn. Matter.* **67** 65
- [15] Anderson P W 1959 *Phys. Rev.* **115** 2
- [16] Bauer B *et al* (ALPS Collaboration) 2011 *J. Stat. Mech.* **P05001**
Albuquerque A F *et al* (ALPS Collaboration) 2007 *J. Magn. Mater.* **310** 1187
- [17] Alet F, Wessel S and Troyer M 2005 *Phys. Rev. E* **71** 036706